ACS Sustainable Chemistry & Engineering

Research Article

pubs.acs.org/journal/ascecg

In-Situ Growth of Few-Layered MoS_2 Nanosheets on Highly Porous Carbon Aerogel as Advanced Electrocatalysts for Hydrogen Evolution Reaction

Youfang Zhang,[†] Lizeng Zuo,[†] Yunpeng Huang,[†] Longsheng Zhang,[†] Feili Lai,[†] Wei Fan,*[,‡] and Tianxi Liu*[,†,‡]

[†]State Key Laboratory of Molecular Engineering of Polymers, Department of Macromolecular Science, Fudan University, 220 Handan Road, Shanghai 200433, P. R. China

[‡]State Key Laboratory of Modification of Chemical Fibers and Polymer Materials, College of Materials Science and Engineering, Donghua University, 2999 North Renmin Road, Shanghai 201620, P. R. China

Supporting Information

ABSTRACT: Molybdenum disulfide-based hybrids, acting as cost-effective and acid-stable electrocatalysts for hydrogen evolution reaction (HER), have been developed fast for providing sustainable hydrogen energy in recent years. Herein, few-layered molybdenum disulfide (MoS_2) nanosheets/carbon aerogel (CA) hybrids were successfully obtained through the combination of sol−gel process, aging, freeze-drying, high temperature carbonization, and solvothermal reaction. CA with highly continuous porosity and high specific surface area is used as a matrix material for construction of hierarchical MoS_2/CA hybrids where few-layered MoS_2 nanosheets are uniformly covered on a CA surface. In this heterostructured system, CAs not only provide three-dimensional (3D) conductive pathway for fast transportation of electrons and ions, but also offer highly active regions for the growth of MoS_2, greatly preventing the aggregation of MoS_2 nanosheets. Due to the rationally designed hybrids with 3D porous nanostructures, the as-prepared MoS_2/CA hybrids with optimized MoS_2 content exhibit enhanced catalytic performance for electrocatalytic HER with a low onset potential of −0.14 V, large current density, and excellent stability.

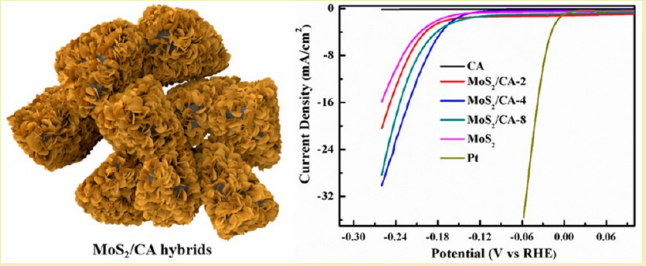

KEYWORDS: *Molybdenum disulfide, Carbon aerogels, Hydrogen evolution reaction*

INTRODUCTION

More and more scientific works have been committed to search for clean and renewable energy alternatives due to the severe stress from global environmental pollution and the energy crisis derived from excessive consumption of fossil fuels.[1−4] Among various energy storage methods, the water splitting reaction excited either by light or electricity for renewable hydrogen energy has attracted tremendous attention because of its cleanliness and potentially low cost.[5−9] The essential step in water electrolysis is the hydrogen evolution reaction (HER), in which hydrogen is generated by electrocatalytic reduction of hydrogen ions.[10−13] Platinum (Pt) and its alloys are very active catalysts for HER owing to their highly efficient energy conversion ability and low overpotential.[14] However, the low natural reserves and expensive cost of Pt- and Pt-based alloys hamper their commercial application in electrochemical hydrogen generation. Transition metal dichalcogenides (TMD) materials, for instance, MoS_2, WS_2, $MoSe_2$, WSe_2, and VSe_2, are developed as potential alternatives of Pt-group electrocatalysts for HER due to their constrained electrons within two-dimensional (2D) layers.[2,15−21]

As a typical 2D TMD layered material, MoS_2 shows graphene-like structure, in which molybdenum atoms are sandwiched between two layers of sulfur atoms. Recently, researchers have found that MoS_2 can be a promising electrocatalyst for HER.[22−31] Liu et al.[32] prepared 2D MoS_2 nanosheets from commercial MoS_2 powder via liquid exfoliation and ultrasonication. The obtained MoS_2 nanosheets exhibited extraordinary HER electrocatalytic performance, with onset potential lowered to −0.12 V. Previous works show that the defective sulfur (S) edges in MoS_2 nanosheets have excellent electrocatalytic activity, which favors the HER process by decreasing the overpotentionals and increasing the current densities. However, the basal planes of MoS_2 are catalytically inert. Therefore, MoS_2 nanosheets with small size and few stacked layers have better electrocatalytic activity because of the existence of more exposed sulfur edge sites. Until now, there are many kinds of preparation methods for the synthesis of nanosized MoS_2, such as chemical vapor deposition, electro-

Received: July 16, 2015
Revised: September 21, 2015
Published: October 26, 2015

DOI: 10.1021/acssuschemeng.5b00700
ACS Sustainable Chem. Eng. 2015, 3, 3140−3148

chemical deposition, hydrothermal reaction, and inverse micelle method. However, another obstacle for the practical application of MoS_2 nanosheets in the HER field is their poor conductivity. Therefore, increasing the conductivity of MoS_2 nanosheets while maintaining their nanosize is the key challenge to realize the practical application of MoS_2 nanosheets in HER. In this regard, preparation of uniformly distributed and edge-rich MoS_2 nanosheets on a conductive substrate is an effective strategy to enhance their catalytic activity for HER.

Carbon materials, including graphene, carbon nanofibers (CNFs), carbon nanotubes (CNTs), activated carbon, carbon papers, and so on, are ideal substrates for loading MoS_2 to advance their electrocatalytic performance due to the excellent conductivity and stability of these carbon materials.[33−40] MoS_2/carbon hybrids have enormous advantages, such as great varieties, high surface-to-volume ratio, tunable molecular structures, and good stability in a harsh environment. For example, Dai et al.[41] first reported few-layer MoS_2 nanosheets with abundant exposed sulfur edges stacked on reduced graphene oxide (rGO) sheets by a selective solvothermal method. In the MoS_2/rGO hybrids, rGO offers the conductive path for electron transfer between the catalyst and electrode, and provides active sites for the growth of MoS_2, which prevents the aggregation of MoS_2 and enhances the exposure of S-edges. Thus, the obtained MoS_2/rGO hybrids show excellent electrocatalytic performance, and the onset overpotential is low to −0.1 V along with a decreased Tafel slope (41 mV/decade). Du et al.[42] reported a novel synthesis of 2D MoS_2 with single layer nanosized nanoplatelets and S-edge-rich by hybridization with one-dimensional (1D) CNFs. The designed hybrids exhibit a decreased overpotential of 300 mV at high current density of 80.3 mA/cm^2 and a low Tafel slope of 42 mV/decade. Wang et al.[43] prepared low crystalline MoS_2 nanosheet coated CNTs which exhibited enhanced catalytic activity for HER. Among various carbon materials, carbon aerogel (CA) with 3D interconnected network and unique properties, including highly porous structure, large surface area, and great electron transport performance, is an ideal substrate for MoS_2 loading and can be used in energy area.[44−46] To our best knowledge, the nanocomposites of MoS_2 nanosheets and CAs have not been previously applied in the field of HER.

In this work, a novel and facile strategy is developed for the fabrication of 3D CA supported MoS_2 nanosheets with the combination of sol−gel process, high temperature carbonization, and solvothermal reaction. CA acting as the 3D conductive substrate can not only prevent the aggregation of MoS_2 and enhance the exposure of active S-edges, but also improve the conductivity of the MoS_2/CA hybrids, thus facilitating electron transfer during the electrocatalysis process. Morphological characterizations show that few-layered MoS_2 nanosheets with abundant edges are vertically grown on the surface of CA substrate uniformly. Owing to the highly exposed edge sites and relatively low aggregation, the obtained MoS_2/CA hybrids exhibit excellent electrocatalytic properties, with a low onset potential of −0.14 V, large current density, and excellent stability, making it a potential electrocatalyst for HER.

EXPERIMENTAL SECTION

Materials. Pyromellitic dianhydride (PMDA), *N*,*N*-dimethylacetamide (DMAc), triethylamine (TEA, 99%), 4,4′-oxidianiline (ODA), 30% H_2O_2, 98% H_2SO_4, $KMnO_4$, 37% HCl, *N*,*N*-dimethylformamide (DMF), ammonium molybdate, and thiourea were obtained from Sinopharm Chemical Reagent Co., Ltd. All the above reagents were used as received without any treatments. Natural graphite powder (325 mesh) was supplied by Alfa-Aesar (Ward Hill, MA) and used without further treatments. All other chemicals were obtained from Aladdin Chemical Reagent, Co., Ltd., and used as received.

Preparation of MoS_2/CA Hybrids. Polyimide (PI)-based CAs (derived from graphene cross-linked PI aerogels) were synthesized according to our methods reported previously.[47] The preparation of MoS_2/CA hybrids is shown in Scheme 1. First of all, the bulk CAs were smashed into powder by continuous ball-milling at 500 rpm for 4 h. MoS_2/CA hybrids with various MoS_2 amounts were synthesized via a one-step solvothermal method according to Xie's method.[28] In brief, proper contents of ammonium molybdate and thiourea with a molar ratio of 1:2 were added to 60 mL water, and this was followed by addition of a certain amount of CAs. Then, the mixture was well-mixed by magnetic stirring for 2 h at room temperature. The obtained dispersion was transferred to a 100 mL Teflon stainless-steel autoclave and reacted at the temperature of 200 °C for 12 h. The precipitates were obtained through centrifugation at 12 000 rpm for 10 min, and then were washed with DI water and anhydrous ethanol several times and finally dried under vacuum at 80 °C for 6 h. Afterward, the samples were calcined at 300 °C for 2 h with a heat rate of 2 °C min^{-1} under N_2 atmosphere. Finally, the MoS_2/CA hybrids with the initial CA/Mo weight ratio of 1:2, 1:4, and 1:8 were obtained and denoted as MoS_2/CA-2, MoS_2/CA-4, and MoS_2/CA-8, respectively. For comparison, pure CA and pure MoS_2 were prepared under the same conditions.

Scheme 1. Schematic for the Preparation of MoS_2/CA Hybrids

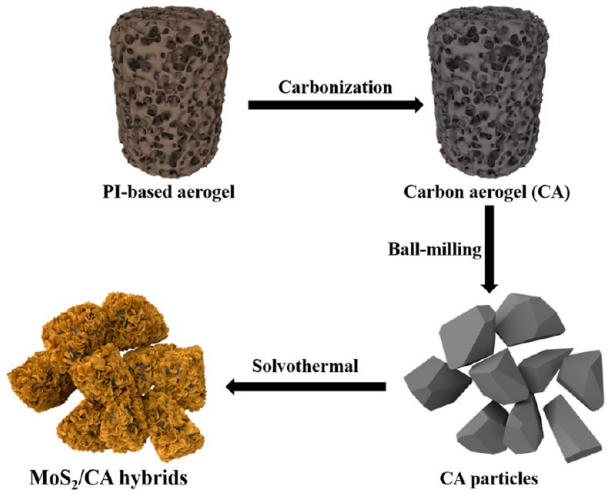

Characterization. The microstructures of the obtained samples were characterized by field emission scanning electron microscopy (FESEM) (Ultra 55, Zeiss) at 5 kV acceleration voltage. The chemical composition was characterized by the energy dispersive X-ray spectroscopy (EDX). Transmission electron microscopy (TEM) and high resolution transmission electron microscopy (HRTEM) observations were conducted with JEOL JEM 2100 TEM under 200 kV acceleration voltage. X-ray diffraction (XRD) patterns were performed on an X'Pert Pro X-ray diffractometer with Cu Kα radiation (λ = 0.1542 nm) under a current of 40 mA and a voltage of 40 kV with 2θ ranges from 5° to 80°. X-ray photoelectron spectroscopy (XPS) analyses were performed with a VG ESCALAB 220I-XL device, and all XPS spectra were corrected using C 1s line at 284.5 eV. In addition, the curve fitting and background subtraction were accomplished using XPS PEAK41 software. In order to calculate the mass content of MoS_2 nanosheets in the hybrids, thermogravimetric analysis (TGA) was used under air flow from 100 to 700 °C at a heating rate of 20 °C/min.

Electrochemical Measurements. Prior to all the experiments of hydrogen evolution performance, glassy carbon electrodes (GCE) of 3 mm in diameter were preprocessed according to the previous report.[21]

DOI: 10.1021/acssuschemeng.5b00700
ACS Sustainable Chem. Eng. 2015, 3, 3140−3148

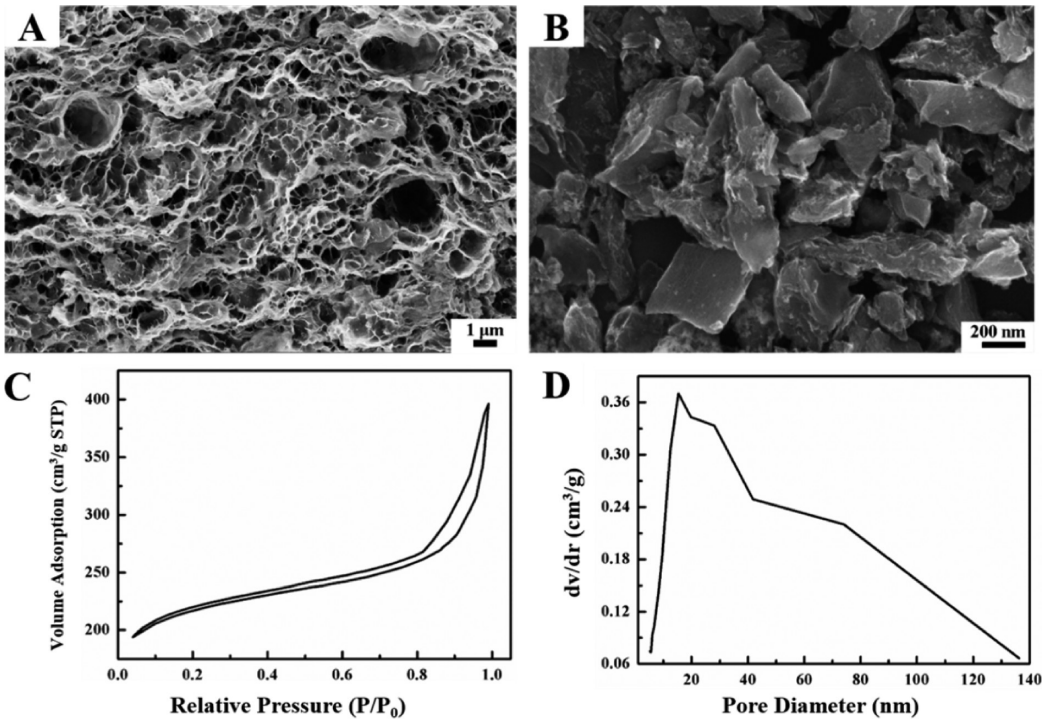

Figure 1. FESEM images of CAs (A) and CA particles (B). N_2 adsorption/desorption isotherm at 77 K (C) and pore size distribution (D) of CAs.

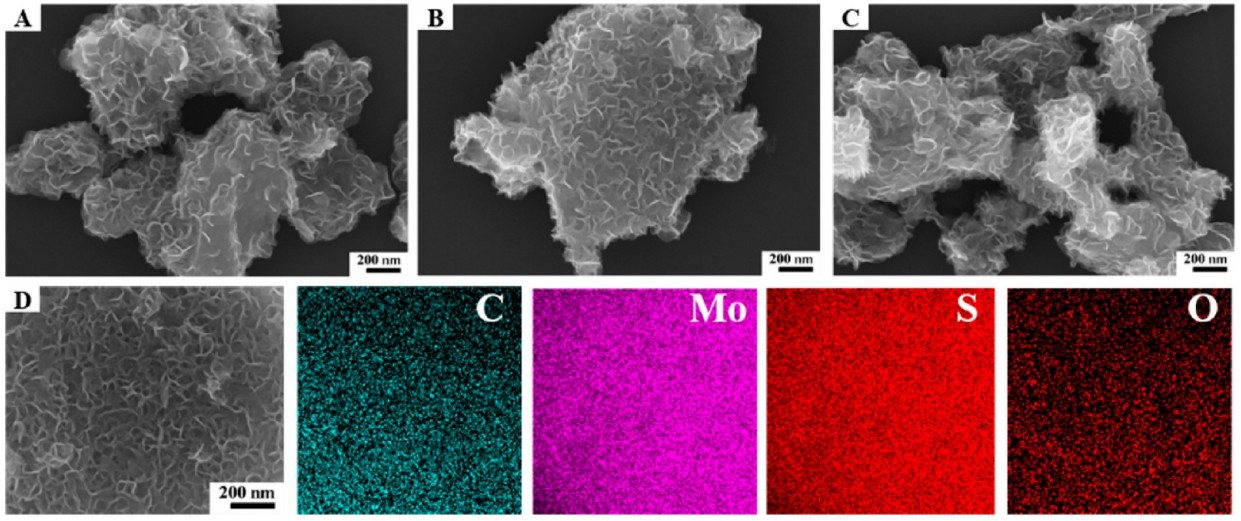

Figure 2. FESEM images of MoS_2/CA-2 (A), MoS_2/CA-4 (B), and MoS_2/CA-8 hybrids (C). The bottom row shows the EDX mapping of MoS_2/CA-4 hybrid (D).

Typically, the working electrode was prepared as follows. A 2 mg portion of MoS_2/CA hybrid was dispersed in 1 mL of a mixed solvent (DMF and deionized water by a volume ratio of 1:1) containing 20 μL 5 wt % nafion. Then, the mixture was sonicated at least 15 min in order to obtain the homogeneous suspension. Finally, 10 μL of the homogeneous mixture was dropped onto GCE to form MoS_2/CA hybrid modified GCE. The required loadings of the electrocatalyst were adjusted by repeatedly adding 5 μL of the obtained MoS_2/CA hybrid slurry.

All electrochemical catalytic reasearch was carried out by a CHI 660D electrochemical workstation (Chenhua Instruments Co, Shanghai, China) at room temperature. The hydrogen evolution performance tests were performed in the electrolyte solution of 0.5 M H_2SO_4. For a standard typical three-electrode cell, the different electrocatalyst modified GCE was applied as the working electrode, with saturated calomel electrode (SCE) as the reference electrode and Pt wire as counter electrode, respectively. In our electrochemical tests, all the potentials were calibrated to RHE according to the equation $E_{RHE} = E_{SCE} + (0.241 + 0.059\ pH)$ V. The electrocatalytic performance of MoS_2/CA hybrid toward HER was performed by linear sweep voltammetry (LSV) in nitrogen purged electrolyte solution, and the scan rate was 2 mV/s. Electrochemical impedance spectroscopy (EIS) measurements were conducted in 0.5 M H_2SO_4 by applying an ac voltage in the frequency range between 100 kHz and 10 mHz with 5 mV amplitude.

RESULTS AND DISCUSSION

Morphology and Structures of MoS_2/CA Hybrids. The typical structure of CA and CA particles after ball-milling is shown in Figure 1. As shown in Figure 1A, the obtained CA possesses high porosity, and the pore sizes range from dozens

DOI: 10.1021/acssuschemeng.5b00700
ACS Sustainable Chem. Eng. 2015, 3, 3140−3148

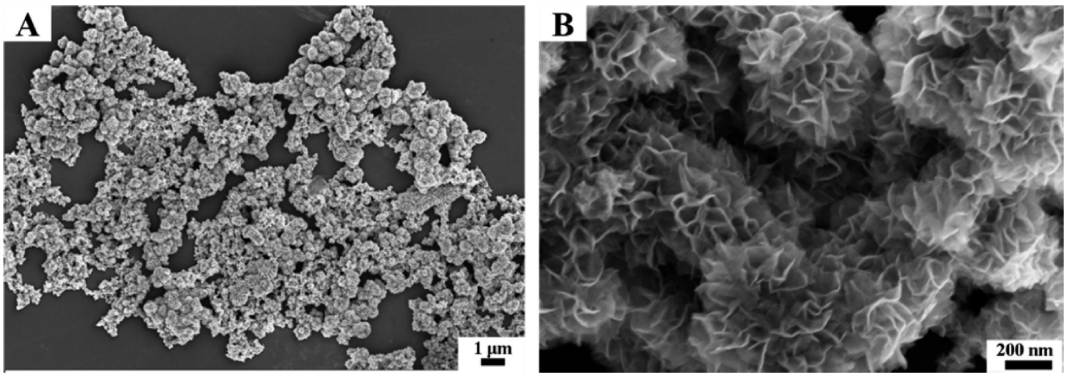

Figure 3. FESEM images of pure MoS_2 at low (A) and high (B) magnifications.

of nanometers to hundreds of nanometers. These porous structures can offer a 3D conductive substrate, which is beneficial for ion and electron transport. Irregular structures with many sharp edges and sizes of hundreds of nanometers are observed for CA particles (Figure 1B). The irregular structure of CA particles favors the growth of MoS_2 nanosheets so that they can not only prevent the agglomeration of MoS_2 nanosheets, but also increase the exposure of the active MoS_2 edges, thus highly improving the catalytic performance for HER. Specific surface area and porous structure of the obtained CA are characterized by nitrogen physisorption isotherms (Figure 1C,D). The specific surface area of CA is 978 m^2/g, and the isotherm curve belongs to type IV with a hysteresis loop, indicating that the CA possesses a large quantity of mesopores. The pore size distribution (in the range 0−140 nm) measured by the Barrett−Joiner−Halenda method presents a relatively narrow distribution, which was centered at 15 nm. Therefore, the obtained CA with large surface area and high porosity is considered as a promising template for further construction of MoS_2/CA hybrids with hierarchical nanostructures.

CAs with different loading amounts of MoS_2 nanosheets were prepared with the same procedure by adjusting the weight ratio of CA/Mo from 1:2, 1:4 to 1:8. After in-situ solvothermal reaction of CA powder in molybdenum salt solution, few-layered MoS_2 nanosheets are evenly grown onto 3D conductive CA substrate (Figure 2A−C). By increasing the loading amount of molybdenum salt, more and more thin MoS_2 nanosheets begin to form and densely grow on the CA particles. It is worth mentioning that MoS_2 nanosheets are evenly and perpendicularly grown on the porous CA substrate when the weight ratio of molybdenum salt precursor to CA is 4:1. However, with increasing the weight ratio of molybdenum salt precursor to CA to 8:1, MoS_2 nanosheets began to accumulate and stack together on CA substrate due to the limited growth space (Figure 2C). The EDX mapping analysis of the MoS_2/CA-4 hybrid (Figure 2D) proves the coexistence and homogeneous dispersion of C, Mo, S elements, further confirming that MoS_2 nanosheets are evenly anchored on the surface of CA particles. In contrast, as shown in Figure 3, pure MoS_2 prepared without adding CA particles consists of large microsized sheets, which are disorderly stacked together and aggregated into nanospheres. In addition, specific surface area and porous structure of the obtained pure MoS_2 and MoS_2/CA-4 hybrid is characterized by nitrogen physisorption isotherms, as shown in Figure S1. The specific surface area of MoS_2/CA-4 hybrid is 107 m^2/g, which is much larger than that of pure MoS_2 (13 m^2/g). The main reason is due to the special structure of CA with high surface area (978 m^2/g) being able to offer more active sites for the growth of MoS_2 nanosheets, which is beneficial for preventing the aggregation of MoS_2 nanosheets. The pore size distribution of pure MoS_2 and MoS_2/CA-4 hybrid calculated by the Barrett−Joiner−Halenda method presents a relatively narrow distribution, which is centered at 4 nm. The high surface area and porous structure of MoS_2/CA-4 hybrid is beneficial for electrolyte permeation and efficient ion diffusion, thus facilitating the HER electrocatalytic performance.

Morphology of MoS_2/CA-4 hybrid is further confirmed by TEM observations (Figure 4). The irregular CA particles are

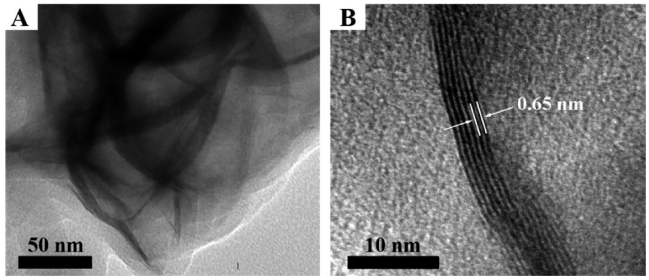

Figure 4. TEM (A) and HRTEM (B) images of MoS_2/CA-4 hybrid.

clearly observed, and few-layered MoS_2 nanosheets are evenly coated on CA substrate, which is in good accordance with SEM observations (Figure 2). From the HRTEM image in Figure 4B, 5−8 layers of MoS_2 nanosheets can be clearly observed, and the interlayer spacing of MoS_2 nanosheets is about 0.65 nm, which is in accordance with the (002) lattice of hexagonal MoS_2.

The XRD patterns of pure CA, pure MoS_2, and MoS_2/CA-4 hybrid are shown in Figure 5. As for CA sample, the broad diffraction peak centered at $2\theta = 26°$ and the weak diffraction peak at $2\theta = 44°$ can be assigned to the (002) and (100) planes, respectively, revealing the low crystalline degree of CA. For pure MoS_2 and MoS_2/CA-4 hybrid, the diffraction peaks present similarly to each other, indicating that no additional crystallization behavior is introduced into the MoS_2/CA-4 hybrid. In addition, all the diffraction peaks of pure MoS_2 and MoS_2/CA-4 hybrid can be indexed to the hexagonal MoS_2 phase, which are in good accordance with the literature values (JCPDS: 00-037-1492). As shown in Figure 5, the MoS_2/CA-4 hybrid shows sharp peaks at $2\theta = 14.2°$, 33.8°, and 59.3°, which can be indexed to (002), (100), and (110) planes of MoS_2, respectively. To emphasize, the diffraction peak of (002) shifted from $2\theta = 16.7°$ to 14.2° as compared to the standard hexagonal 2H-MoS_2 structure, indicating an expanded inter-

DOI: 10.1021/acssuschemeng.5b00700
ACS Sustainable Chem. Eng. 2015, 3, 3140−3148

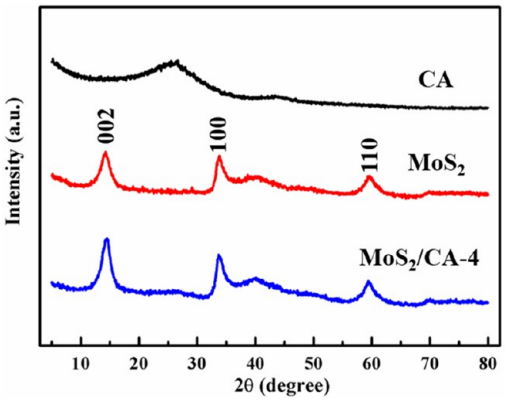

Figure 5. XRD patterns of pure CA, pure MoS_2 nanosheets, and MoS_2/CA-4 hybrid.

layer. In addition, the (103) and (201) peaks at $2\theta = 39.8°$ and 69.8° can be weakly detected. Therefore, the XRD results suggest that MoS_2 has been successfully grown on the surface of CA.

Figure 6 shows the XPS spectra of the MoS_2/CA-4 hybrid. As shown in Figure 6A, the survey scan indicates that C, Mo, S, and O elements coexist in the MoS_2/CA-4 hybrid. The peak of C 1s spectrum is centered at 284.5 eV, which corresponds to sp^2 C (Figure 6B). High resolution Mo 3d spectrum (Figure 6C) shows characteristic peaks centered at 232.3 and 229.2 eV corresponding to Mo $3d_{3/2}$ and Mo $3d_{5/2}$ orbitals, suggesting that Mo in the MoS_2/CA-4 hybrid is in the Mo(IV) state. In addition, the binding energies of S $2p_{1/2}$ and S $2p_{3/2}$ orbitals were centered at 163.1 and 162.0 eV, indicating the existence of divalent sulfide ions (S^{2-}) (Figure 6D). The loading amounts of MoS_2 in the MoS_2/CA hybrids are calculated from the TGA curves (Figure 7), which is 21.6%, 38.4%, and 68.1% for MoS_2/CA-2, MoS_2/CA-4, and MoS_2/CA-8 hybrids, respectively.

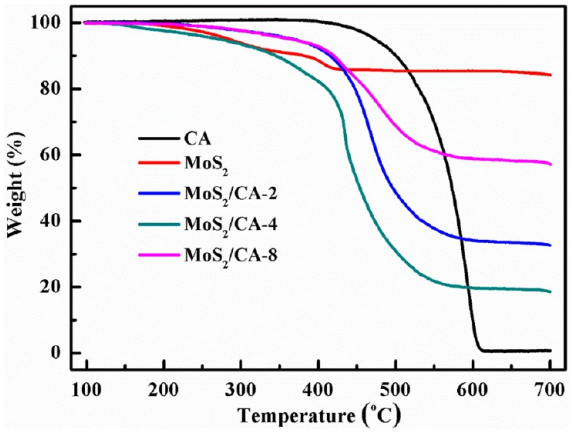

Figure 7. TGA curves of pure CA, pure MoS_2, and MoS_2/CA hybrids.

Electrochemical Performance of MoS_2/CA Hybrids. Generally speaking, an optimal HER catalyst is a material that could give the highest current at the lowest overpotential, as well as a low HER onset potential (i.e., the potential at which HER activity begins) comparable to that of Pt catalyst. The electrocatalytic performance of the MoS_2/CA hybrids for HER were carried out in the electrolyte solution of 0.5 M H_2SO_4 using a standard typical three-electrode cells. Typically, the hybrids with an optimized electrocatalyst loading weight of 20 μg were deposited on GCE. The polarization curves for all the hybrids were optimized, and commercial Pt/C catalysts, pure CA, and pure MoS_2 were also measured as reference (Figure 8). As shown in Figure 8A, either CA or pure MoS_2 exhibits no or

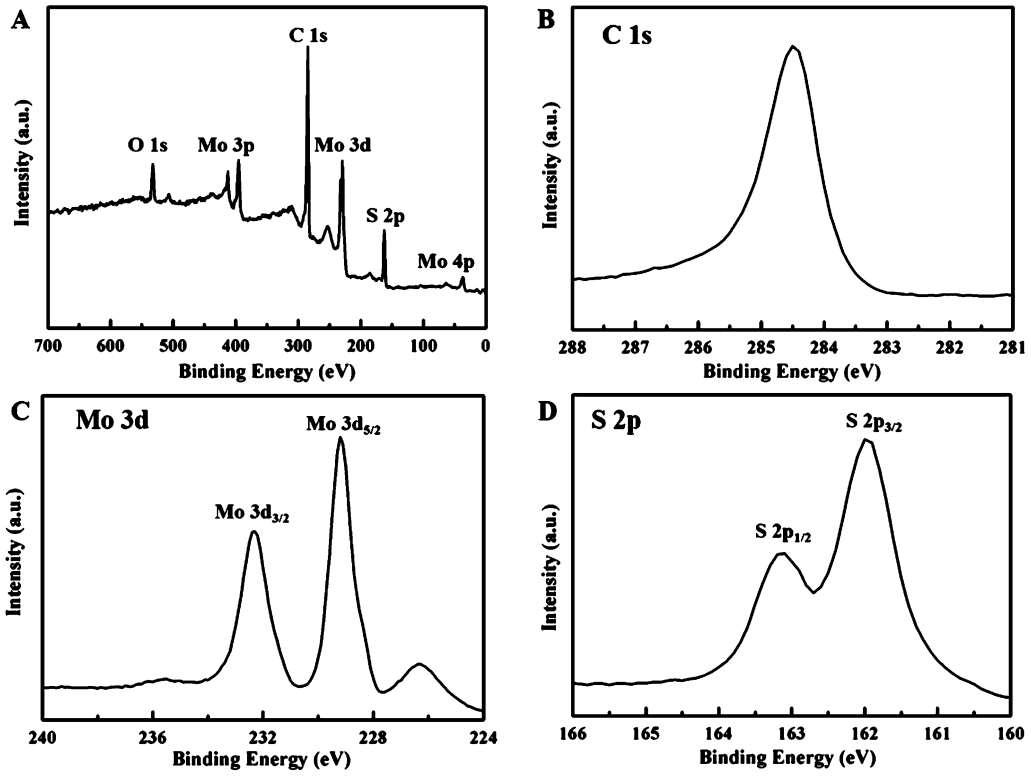

Figure 6. XPS survey spectrum (A), C 1s spectrum (B), Mo 3d spectrum (C), and S 2p spectrum (D) of MoS_2/CA-4 hybrid.

DOI: 10.1021/acssuschemeng.5b00700
ACS Sustainable Chem. Eng. 2015, 3, 3140−3148

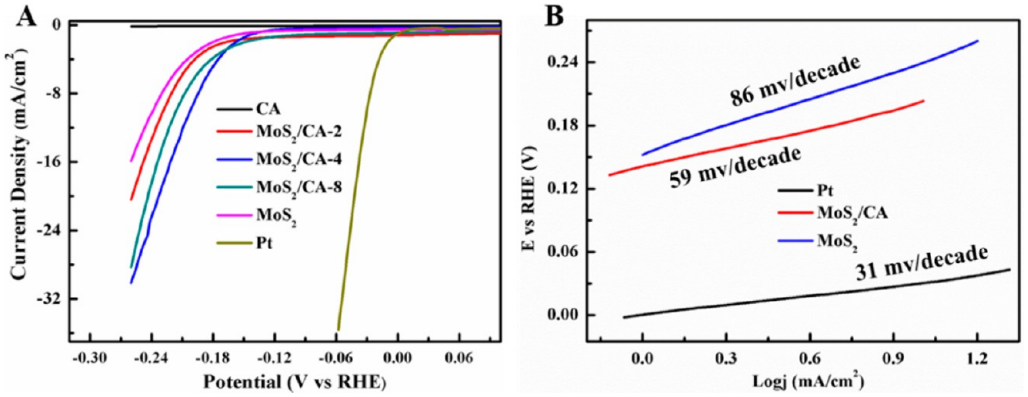

Figure 8. LSV polarization curves for GCE modified with different materials in N_2 purged 0.5 M H_2SO_4 solution (A). Scan rate: 2 mV/s. Tafel plots for pure MoS_2 nanosheets, Pt, and MoS_2/CA-4 modified GCE (B).

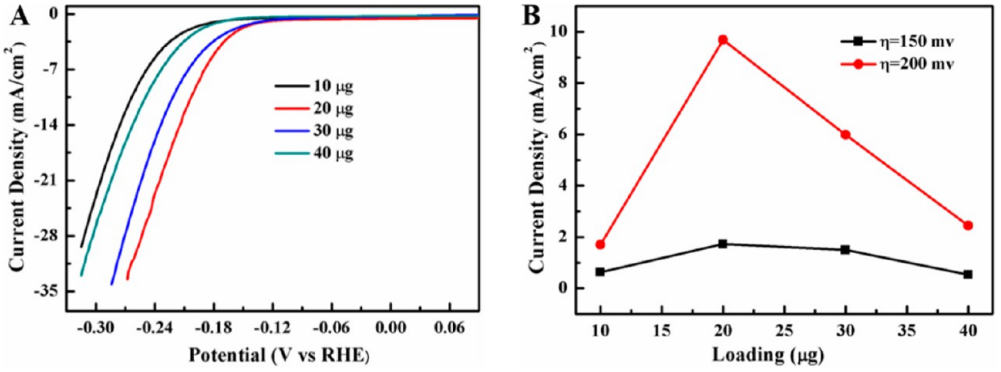

Figure 9. LSV polarization curves for MoS_2/CA-4 modified GCE with different loadings in N_2 purged 0.5 M H_2SO_4 solution (A). Scan rate: 2 mV/s. Current densities for MoS_2/CA-4 modified GCE with various loadings at overpotentials of 150 and 200 mV (B).

poor HER electrocatalytic performance due to the large onset overpotential and low current densities. All three MoS_2/CA hybrids with different Mo/CA ratios do have good electrocatalytic activity, while MoS_2/CA-4 hybrid exhibits the optimized electrocatalytic performance, with onset potential at approximately −0.14 V (vs RHE), and high current densities of 1.72 and 9.68 mA/cm^2 at overpotentials of 150 and 200 mV, respectively. The improved electrocatalytic HER activity for MoS_2/CA hybrids suggests the synergistic effect between 3D conductive CAs and electroactive MoS_2 nanosheets. As mentioned above, highly porous CA provides 3D conductive templates, which are conductive to reduce the diffusion path for ions and electrons. Besides, the distinctive structures of CA particles are able to offer many active sites for the homogeneous growth of MoS_2 nanosheets and thus prevent the self-aggregation of MoS_2 nanosheets. Furthermore, the irregular shape of CA particles can provide many sharp edges, maximizing the exposure of accessible active catalytic sites of MoS_2 nanosheets. For MoS_2/CA-2 hybrid, only sparse MoS_2 nanosheets are interspersed on the surface of CA particles, leading to less electroactive sites for hydrogen evolution. In contrast, as for the MoS_2/CA-8 hybrid, excess loading of MoS_2 nanosheets could result in the aggregation of MoS_2 nanosheets, limiting the exposure of MoS_2 edges and electroactive sites. Therefore, with uniform distribution of MoS_2 nanosheets and 3D conductive network of CA template, MoS_2/CA-4 hybrids show synergistically improved catalytic performance for HER.

A Tafel slope is closely related to reaction path and adsorption type during the HER process. Therefore, it is always used to evaluate the catalytic effectiveness of catalysts. Usually, the Tafel curve derived from the polarization curves is obtained on the basis of fitting of the straight line part, and the Tafel slope is the slope of the fitting line. For the Tafel curve, the overpotential (η) and the relevant current density (j) are obtained from the LSV curves. The linear portions of the Tafel curve agree with the Tafel equation ($\eta = b \log(j) + a$, where η is the overpotential, j is the current density, and b is the Tafel slope) at different overpotential ranges. The Tafel curves for pure MoS_2, MoS_2/CA-4 hybrid, and Pt, obtained from the LSV curves, are shown in Figure 8B. As calculated from Figure 8B, the Tafel slopes are ∼86, ∼59, and ∼31 mV/decade for pure MoS_2, MoS_2/CA-4 hybrid, and Pt, respectively. Compared to pure MoS_2, the improved HER performance of the MoS_2/CA-4 hybrid suggests a smaller activation energy for HER, which can be attributed to the effective hybridization of 3D electrical conductive CA and the homogeneous, nanosized, and S-edge-rich MoS_2 nanosheets. According to the typical electrocatalytic mechanism in acidic aqueous for HER, the rate-determining step of the obtained pure MoS_2 belongs to the Volmer reaction due to the intrinsic poor conductivity and low activity that arose from its microsize and disordered stacking. The evidently reduced slope for MoS_2/CA-4 hybrid indicates that the hydrogen evolution takes place via the rapid Volmer reaction followed by a rate-determining Heyrovsky step.

Figure 9 shows the HER catalytic performance of different loadings of MoS_2/CA-4 hybrid on GCE. As shown in Figure 9A,B, the optimal loading of MoS_2/CA-4 hybrid is 20 μg with current densities of 1.72 and 9.68 mA/cm^2 at overpotentials of 150 and 200 mV, respectively. For 30 and 40 μg loadings, the current densities at different overpotentials are lower than that

DOI: 10.1021/acssuschemeng.5b00700
ACS Sustainable Chem. Eng. 2015, 3, 3140−3148

of 20 μg loading, which may be explained by the observation that excess loading of catalyst will increase the internal resistance and decrease the effective active sites.

In order to assess the electrode kinetics and electrical conductivity of the different electrocatalysts, EIS of pure CA, pure MoS_2, and MoS_2/CA hybrids were measured from 0.01 to 100 000 Hz. As can be seen from Figure 10, the Nyquist plots

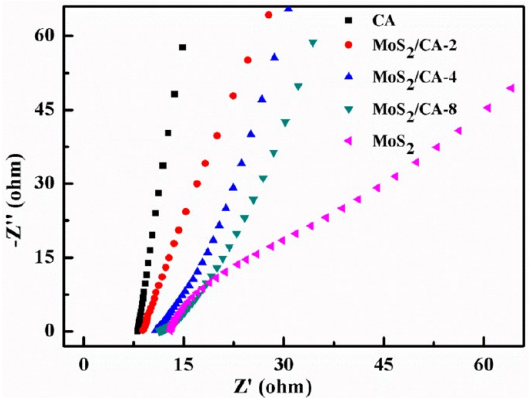

Figure 10. Alternating current impedance spectroscopy of CAs, pure MoS_2 nanosheets, and MoS_2/CA hybrids in 0.5 M H_2SO_4 from 10^{-2} to 10^5 Hz with an ac amplitude of 5 mV.

of the catalyst modified electrodes consist of an inconspicuous arc in the high frequency region and a straight line with a certain slope in the low frequency region. According to the previous reports, the more vertical the line is, the faster ions diffuse at low frequency. It is clear that pure CA has a more vertical curve due to its good conductivity, which is conducive to fast ion and electron transport.[47] Besides, all three of the MoS_2/CA hybrids have more vertical curves than pure MoS_2, indicating that MoS_2/CA hybrids offer faster HER kinetics due to the 3D conductive CA template. For the high frequency area, the solution resistance (R_s) of pure CA, MoS_2/CA-2, MoS_2/CA-4, MoS_2/CA-8 hybrid and pure MoS_2 are about 8.1, 8.9, 10.8, 11.4, and 13.0 Ω, respectively. The reduced R_s value for MoS_2/CA hybrids compared with that of pure MoS_2 indicates the improved electrical conductivity result from the effective hybridization of MoS_2 with porous CA, which can efficiently shorten the transport path of ions and charges due to its 3D porous structure. With the weight ratio of the molybdenum salt precursor to CA increased, it is clear that the values of R_s become larger and the constant inclining angle of the straight line is smaller, indicating increased internal resistance with the excess loading of MoS_2. In addition, ac impedance spectroscopy of MoS_2/CA-4 hybrid in 0.5 M H_2SO_4 from 10^{-2} to 10^5 Hz under different overpotentials was investigated. As shown in Figure S2, there is almost no difference among the ac impedance spectroscopy of MoS_2/CA-4 hybrid under different overpotentials, and this phenomenon shows that the conductivity of MoS_2/CA-4 hybrid is stable under the potential range of hydrogen evolution.

To evaluate the long-term stability of the MoS_2/CA-4 hybrid, potential sweeps were carried out continuously for 2000 cycles from −0.4 to +0.2 V versus RHE. As seen from Figure 11, the LSV curves of MoS_2/CA-4 hybrid stay similar before and after 2000 continuous cycles, indicating that it has good durability. To further investigate the stability of MoS_2/CA hybrids in HER, the current−time plots (I−T curves) at different potentials (to achieve 10 mA/cm^2) were examined. As shown

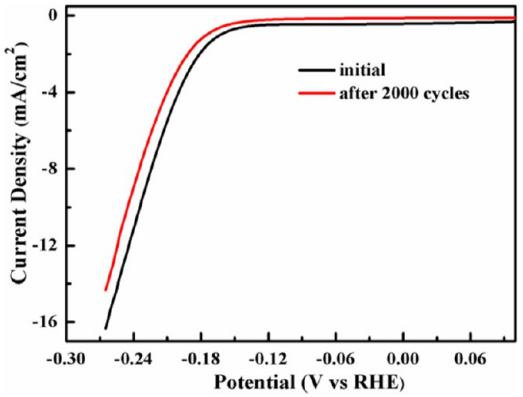

Figure 11. Polarization curves of MoS_2/CA-4 hybrid in 0.5 M H_2SO_4 initially and after 2000 cycles between −0.4 and +0.2 V at 100 mV/s.

in Figure S3, all the catalytic current densities slightly fluctuated up and down due to the bubble formation in the process. Besides, with increasing the weight ratio of molybdenum salt precursor to CA, the current density reduced faster while MoS_2/CA hybrid needs higher voltage to ensure the current density due to the decrease of conductivity with fewer CA particles.

CONCLUSIONS

In summary, a highly active electrocatalyst of MoS_2/CA hybrid was fabricated where MoS_2 nanosheets were grown uniformly on 3D mesoporous CA template by a simple solvothermal reaction. CA has abundant mesopores, a high surface area, and a highly conductive skeleton which provide a specific microenvironment and conductive pathways to accelerate the transportation of electrons and ions during the HER process. Besides, CA acting as conductive substrate can effectively prevent the aggregation of MoS_2 nanosheets, and thus, the well-dispersed and edge-rich MoS_2 nanosheets grown on CA template guarantee the full exposure of active edge sites. Therefore, the obtained MoS_2/CA-4 hybrid possesses excellent catalyst performance for HER with a low onset potential of −0.14 V, large current densities (1.72 mA/cm^2 at η = 150 mV; 9.68 mA/cm^2 at η = 200 mV, relatively), and a small Tafel slope of 59 mV/decade. Besides, the MoS_2/CA-4 hybrid shows long-term durability after 2000 cycles. Therefore, the highly electrocatalytically active CA supported nanosized MoS_2 is a promising candidate for low cost electrocatalysts in hydrogen evolution field.

ASSOCIATED CONTENT

Supporting Information

The Supporting Information is available free of charge on the ACS Publications website at DOI: 10.1021/acssuschemeng.5b00700.

N_2 adsorption−desorption analysis, ac impedance spectroscopy of MoS_2/CA-4 hybrid under different overpotentials, current−time responses of MoS_2/CA hybrids, and LSV polarization curves for MoS_2/CA-4 hybrid at different scan rates (PDF)

AUTHOR INFORMATION

Corresponding Authors

*E-mail: 10110440003@fudan.edu.cn.

DOI: 10.1021/acssuschemeng.5b00700
ACS Sustainable Chem. Eng. 2015, 3, 3140−3148

*E-mail: txliu@fudan.edu.cn. Phone: +86-21-55664197. Fax: +86-21-65640293

Notes

The authors declare no competing financial interest.

■ ACKNOWLEDGMENTS

The authors are grateful for the financial support from the National Natural Science Foundation of China (51125011, 51433001).

■ REFERENCES

(1) Zheng, X. L.; Xu, J. B.; Yan, K. Y.; Wang, H.; Wang, Z. L.; Yang, S. H. Space-Confined Growth of MoS_2 Nanosheets within Graphite: the Layered Hybrid of MoS_2 and Graphene as An Active Catalyst for Hydrogen Evolution Reaction. *Chem. Mater.* **2014**, *26*, 2344−2353.

(2) Chang, Y. H.; Lin, C. T.; Chen, T. Y.; Hsu, C. L.; Lee, Y. H.; Zhang, W. J.; Wei, K. H.; Li, L. J. Highly Efficient Electrocatalytic Hydrogen Production by MoS_x Grown on Graphene-Protected 3D Ni Foams. *Adv. Mater.* **2013**, *25*, 756−760.

(3) Lee, J. H.; Jang, W. S.; Han, S. W.; Baik, H. K. Efficient Hydrogen Evolution by Mechanically Strained MoS_2 Nanosheets. *Langmuir* **2014**, *30*, 9866−9873.

(4) Shin, S.; Jin, Z. Y.; Kwon, D. H.; Bose, R.; Min, Y. High Turnover Frequency of Hydrogen Evolution Reaction on Amorphous MoS_2 Thin Film Directly Grown by Atomic Layer Deposition. *Langmuir* **2015**, *31*, 1196−1202.

(5) Jaramillo, T. F.; Jorgensen, K. P.; Bonde, J.; Nielsen, J. H.; Horch, S.; Chorkendorff, I. Identification of Active Edge Sites for Electrochemical H_2 Evolution from MoS_2 Nanocatalysts. *Science* **2007**, *317*, 100−102.

(6) Danilovic, N.; Subbaraman, R.; Strmcnik, D.; Chang, K.; Paulikas, A. P.; Stamenkovic, V. R.; Markovic, N. M. Enhancing the Alkaline Hydrogen Evolution Reaction Activity through the Bifunctionality of $Ni(OH)_2$/Metal Catalysts. *Angew. Chem., Int. Ed.* **2012**, *51*, 12495−12498.

(7) Dai, T. Y.; Wang, H. J.; Cao, Y.; Lu, Y. Preparation, Characterization and Application of Polyaniline/Epoxide Polysiloxane Composite Films. *Chin. J. Polym. Sci.* **2015**, *33*, 732−742.

(8) Ding, Q. W.; Liu, M. K.; Miao, Y. E.; Huang, Y. P.; Liu, T. X. Electrospun Nickel-Decorated Carbon Nanofiber Membranes as Efficient Electrocatalysts for Hydrogen Evolution Reaction. *Electrochim. Acta* **2015**, *159*, 1−7.

(9) Hong, D.; Yamada, Y.; Sheehan, M.; Shikano, S.; Kuo, C. H.; Tian, M.; Tsuang, C. K.; Fukuzunmi, S. Mesoporous Nickel Ferrites with Spinel Structure Prepared by an Aerosol Spray Pyrolysis Method for Photocatalytic Hydrogen Evolution. *ACS Sustainable Chem. Eng.* **2014**, *2*, 2588−2594.

(10) Walter, M. G.; Warren, E. L.; McKone, J. R.; Boettcher, S. W.; Mi, Q. X.; Santori, E. A.; Lewis, N. S. Solar Water Splitting Cells. *Chem. Rev.* **2010**, *110*, 6446−6473.

(11) Hinnemann, B.; Moses, P. G.; Bonde, J.; Jørgensen, K. P.; Nielsen, J. H.; Horch, S.; Chorkendorff, I.; Nørskov, J. K. Biomimetic Hydrogen Evolution: MoS_2 Nanoparticles as Catalyst for Hydrogen Evolution. *J. Am. Chem. Soc.* **2005**, *127*, 5308−5309.

(12) Voiry, D.; Salehi, M.; Silva, R.; Fujita, T.; Chen, M.; Asefa, T.; Shenoy, V. B.; Eda, G.; Chhowalla, M. Conducting MoS_2 Nanosheets as Catalysts for Hydrogen Evolution Reaction. *Nano Lett.* **2013**, *13*, 6222−6227.

(13) Yan, K.; Wu, G. S. Titanium Dioxide Microsphere-Derived Materials for Solar Fuel Hydrogen Generation. *ACS Sustainable Chem. Eng.* **2015**, *3*, 779−791.

(14) Greeley, J.; Jaramillo, T. F.; Bonde, J.; Chorkendorff, I. B.; Norskov, J. K. Computational High-Throughput Screening of Electrocatalytic Materials for Hydrogen Evolution. *Nat. Mater.* **2006**, *5*, 909−913.

(15) Tan, Y. W.; Liu, P.; Chen, L. Y.; Cong, W. T.; Ito, Y.; Han, J. H.; Guo, X. W.; Tang, Z.; Fujita, T.; Hirata, A.; Chen, M. W. Monolayer MoS_2 Films Supported by 3D Nanoporous Metals for High-efficiency Electrocatalytic Hydrogen Production. *Adv. Mater.* **2014**, *26*, 8023−8028.

(16) Kong, D. S.; Wang, H. T.; Cha, J. J.; Pasta, M.; Koski, K. J.; Yao, J.; Cui, Y. Synthesis of MoS_2 and $MoSe_2$ Films with Vertically Aligned Layers. *Nano Lett.* **2013**, *13*, 1341−1347.

(17) Ramsurn, H.; Gupta, R. B. Nanotechnology in Solar and Biofuels. *ACS Sustainable Chem. Eng.* **2013**, *1*, 779−797.

(18) Jung, Y.; Shen, J.; Sun, Y.; Cha, J. J. Chemically Synthesized Heterostructures of Two-Dimensional Molybdenum/Tungsten-Based Dichalcogenides with Vertically Aligned Layers. *ACS Nano* **2014**, *8*, 9550−9557.

(19) Xu, K.; Wang, F. M.; Wang, Z. X.; Zhan, X. Y.; Wang, Q. S.; Cheng, Z. Z.; Safdar, M.; He, J. Electrochemical Tuning of MoS_2 Nanoparticles on Three-Dimensional Substrate for Efficient Hydrogen Evolution. *ACS Nano* **2014**, *8*, 8468−8476.

(20) Xing, Z. C.; Liu, Q.; Asiri, A. M.; Sun, X. P. High-Efficiency Electrochemical Hydrogen Evolution Catalyzed by Tungsten Phosphide Submicroparticles. *ACS Catal.* **2015**, *5*, 145−149.

(21) Huang, Y. P.; Miao, Y. E.; Zhang, L. S.; Tjiu, W. W.; Pan, J. S.; Liu, T. X. Synthesis of Few-Layered MoS_2 Nanosheet-Coated Electrospun SnO_2 Nanotube Heterostructures for Enhanced Hydrogen Evolution Reaction. *Nanoscale* **2014**, *6*, 10673−10679.

(22) Zhang, L.; Wu, H. B.; Yan, Y.; Wang, X.; Lou, X. W. D. Hierarchical MoS_2 microboxes constructed by nanosheets with enhanced electrochemical properties for lithium storage and water splitting. *Energy Environ. Sci.* **2014**, *7*, 3302−3306.

(23) Zhou, W. J.; Hou, D. M.; Sang, Y. H.; Yao, S. H.; Zhou, J.; Li, G. Q.; Li, L. G.; Liu, H.; Chen, S. W. MoO_2 nanobelts@nitrogen self-doped MoS_2 nanosheets as effective electrocatalysts for hydrogen evolution reaction. *J. Mater. Chem. A* **2014**, *2*, 11358−11364.

(24) Wang, Z.; Hou, J. G.; Yang, C.; Jiao, S. Q.; Zhu, H. M. Three-Dimensional MoS_2-CdS-gamma-TaON Hollow Composites for Enhanced Visible-Light-Driven Hydrogen Evolution. *Chem. Commun.* **2014**, *50*, 1731−1734.

(25) Yang, L. J.; Zhou, W. J.; Hou, D. M.; Zhou, K.; Li, G. Q.; Tang, Z. H.; Li, L. G.; Chen, S. W. Porous metallic MoO_2-supported MoS_2 nanosheets for enhanced electrocatalytic activity in the hydrogen evolution reaction. *Nanoscale* **2015**, *7*, 5203−5208.

(26) Vrubel, H.; Hu, X. Growth and Activation of An Amorphous Molybdenum Sulfide Hydrogen Evolving Catalyst. *ACS Catal.* **2013**, *3*, 2002−2011.

(27) Li, Y. P.; Yu, Y. F.; Huang, Y. F.; Nielsen, R. A.; Goddard, W. A.; Li, Y.; Cao, L. Y. Engineering the Composition and Crystallinity of Molybdenum Sulfide for High-performance Electrocatalytic Hydrogen Evolution. *ACS Catal.* **2015**, *5*, 448−455.

(28) Xie, J. F.; Zhang, H.; Li, S.; Wang, R. X.; Sun, X.; Zhou, M.; Zhou, J. F.; Lou, X. W. D.; Xie, Y. Defect-rich MoS2 Ultrathin Nanosheets with Additional Active Edge Sites for Enhanced Electrocatalytic Hydrogen Evolution. *Adv. Mater.* **2013**, *25*, 5807−5813.

(29) Liao, L.; Zhu, J.; Bian, X. J.; Zhu, L.; Scanlon, M. D.; Girault, H. H.; Liu, B. H. MoS_2 Formed on Mesoporous Graphene as A Highly Active Catalyst for Hydrogen Evolution. *Adv. Funct. Mater.* **2013**, *23*, 5326−5333.

(30) Wang, H. T.; Lu, Z. Y.; Kong, D. S.; Sun, J.; Hymel, T. M.; Cui, Y. Electrochemical Tuning of MoS_2 Nanoparticles on Three-Dimensional Substrate for Efficient Hydrogen Evolution. *ACS Nano* **2014**, *8*, 4940−4947.

(31) Lukowski, M. A.; Daniel, A. S.; Meng, F.; Forticaux, A.; Li, L. S.; Jin, S. Enhanced Hydrogen Evolution Catalysis from Chemically Exfoliated Metallic MoS_2 Nanosheets. *J. Am. Chem. Soc.* **2013**, *135*, 10274−10277.

(32) Ji, S. S.; Yang, Z.; Zhang, C.; Liu, Z. Y.; Tjiu, W. W.; Phang, I. Y.; Zhang, Z.; Pan, J. S.; Liu, T. X. Exfoliated MoS_2 Nanosheets as Efficient Catalysts for Electrochemical Hydrogen Evolution. *Electrochim. Acta* **2013**, *109*, 269−275.

DOI: 10.1021/acssuschemeng.5b00700
ACS Sustainable Chem. Eng. 2015, 3, 3140−3148

(33) Xia, B. Y.; Yan, Y.; Wang, X.; Lou, X. W. D. Recent progress on graphene-based hybrid electrocatalysts. *Mater. Horiz.* **2014**, *1*, 379−399.
(34) Zhou, W. J.; Zhou, K.; Hou, D. M.; Liu, X. J.; Li, G. Q.; Sang, Y. H.; Liu, H.; Li, L. G.; Chen, S. W. Three-Dimensional Hierarchical Frameworks Based on MoS_2 Nanosheets Self-assembled on graphene oxide for efficient electrocatalytic hydrogen evoltion. *ACS Appl. Mater. Interfaces* **2014**, *6*, 21534−21540.
(35) Ma, C. B.; Qi, X. Y.; Chen, B.; Bao, S. Y.; Yin, Z. Y.; Wu, X. J.; Luo, Z. M.; Wei, J.; Zhang, H. L.; Zhang, H. MoS_2 Nanoflower-Decorated Reduced Graphene Oxide Paper for High-Performance Hydrogen Evolution Reaction. *Nanoscale* **2014**, *6*, 5624−5629.
(36) Yu, X. Y.; Hu, H.; Wang, Y. W.; Chen, H. Y.; Lou, X. W. D. Ultrathin MoS_2 nanosheets supported on N-doped carbon nanoboxes with enhanced lithium storage and electrocatalytic properties. *Angew. Chem., Int. Ed.* **2015**, *54*, 7395−7398.
(37) Bian, X. J.; Zhu, J.; Liao, L.; Scanlon, M. D.; Ge, P. Y.; Ji, C.; Girault, H. H.; Liu, B. H. Nanocomposite of MoS_2 on Ordered Mesoporous Carbon Nanospheres: A Highly Active Catalyst for Electrochemical Hydrogen Evolution. *Electrochem. Commun.* **2012**, *22*, 128−132.
(38) Pu, Z. H.; Liu, Q.; Asiri, A. M.; Obaid, A. Y.; Sun, X. P. Graphene Film-Confined Molybdenum Sulfide Nanoparticles: Facile One-step Electrodeposition Preparation and Application as a Highly Active Hydrogen Evolution Reaction Electrocatalyst. *J. Power Sources* **2014**, *263*, 181−185.
(39) Zhao, X.; Zhu, H.; Yang, X. R. Amorphous Carbon Supported MoS_2 Nanosheets as Effective Catalysts for Electrocatalytic Hydrogen Evolution. *Nanoscale* **2014**, *6*, 10680−10685.
(40) Xu, X.; Fan, Z. Y.; Yu, X. Y.; Ding, S. J.; Yu, D. M.; Lou, X. W. D. A nanosheets-on-channel architecture constructed from MoS_2 and CMK-3 for high-capacity and long-cycle-life lithium storage. *Adv. Energy Mater.* **2014**, *4*, 1400902.
(41) Li, Y. G.; Wang, H. L.; Xie, L. M.; Liang, Y. Y.; Hong, G. S.; Dai, H. J. MoS_2 Nanoparticles Grown on Graphene: An Advanced Catalyst for the Hydrogen Evolution Reaction. *J. Am. Chem. Soc.* **2011**, *133*, 7296−7299.
(42) Zhu, H.; Lyu, F. L.; Du, M. L.; Zhang, M.; Wang, Q. F.; Yao, J. M.; Guo, B. C. Design of Two-dimensional, Ultrathin MoS_2 Nanoplates Fabricated within One-Dimensional Carbon Nanofibers with Thermosensitive Morphology: High-Performance Electrocatalysts for the Hydrogen Evolution Reaction. *ACS Appl. Mater. Interfaces* **2014**, *6*, 22126−22137.
(43) Yan, Y.; Ge, X. M.; Liu, Z. L.; Wang, J. Y.; Lee, J. M.; Wang, X. Facile Synthesis of Low Crystalline MoS_2 Nanosheet-Coated CNTs for Enhanced Hydrogen Evolution Reaction. *Nanoscale* **2013**, *5*, 7768−7771.
(44) Liu, R. L.; Wan, L.; Liu, S. Q.; Pan, L. X.; Wu, D. Q.; Zhao, D. An Interface-Induced Co-Assembly Approach towards Ordered Mesoporous Carbon/Graphene Aerogel for High-Performance Supercapacitors. *Adv. Funct. Mater.* **2015**, *25*, 526−533.
(45) Antonietti, M.; Fechler, N.; Fellinger, T. Carbon Aerogels and Monoliths: Control of Porosity and Nanoarchitecture via Sol-Gel Routes. *Chem. Mater.* **2014**, *26*, 196−210.
(46) Li, Y. Q.; Samad, Y. A.; Polychronopoulou, K.; Alhassan, S. M.; Liao, K. Carbon Aerogel from Winter Melon for Highly Efficient and Recyclable Oils and Organic Solvents Absorption. *ACS Sustainable Chem. Eng.* **2014**, *2*, 1492−1497.
(47) Zhang, Y. F.; Fan, W.; Huang, Y. P.; Zhang, C.; Liu, T. X. Graphene/Carbon Aerogels Derived from Graphene Crosslinked Polyimide as Electrode Materials for Supercapacitors. *RSC Adv.* **2015**, *5*, 1301−1308.

DOI: 10.1021/acssuschemeng.5b00700
ACS Sustainable Chem. Eng. 2015, 3, 3140−3148